The Third International Bridge Seismic Workshop, 3rd IBSW
Seattle, Washington, USA - October 1st to 4th, 2019

EXPERIMENTAL INVESTIGATION OF LOW FLEXURAL STRENGTH BRIDGE PIERS WITH UHPC JACKETS

T. Tong[(1)], S.Yuan[(3)], Z. Liu[(2)]

[(1)] Assistant Professor,School of Civil Engineering, Southeast University, Nanjing 210018, PR China, Email: tengtong@seu.edu.cn
[(2)] Professor,School of Civil Engineering, Southeast University, Nanjing 210018, PR China, Email: mr.liuzhao@seu.edu.cn
[(2)] Doctoral candidate of Civil Engineering, Southeast University, Nanjing 210018, PR China, Email: 230179444@seu.edu.cn

Abstract

The effectiveness of an innovative retrofitting method using ultrahigh-performance concrete (UHPC) jackets on the bridge piers with low flexural strength was investigated. Cyclic loading test was performed on the piers, two of which were retrofitted with the mono-wide-strip UHPC (W-UHPC) jacket, and another two were retrofitted with the multi-narrow-strip UHPC (N-UHPC) jacket. Their seismic responses were compared, in terms of damage evolution, hysteretic curve, skeleton curve, ductility and energy dissipation, etc. The piers retrofitted with the W-UHPC jacket owned a higher lateral strength, but were prone to plastic hinge relocation. On the other aspect, N-UHPC jacket improved the retrofitted piers' ductility and smeared concrete damage. Nevertheless, retrofitting quality was crucial to guarantee the tight contact between the multiple UHPC strips and the shaft. Both W- and N- UHPC jackets mitigated residual drift and concrete damage, and thereby enhancing the piers' seismic resilience. The three retrofitting mechanisms from the UHPC jackets are discussed, namely passive confinement effect, cross-section enlargement effect, gap-opening effect, and interface-opening effect.

Keywords: UHPC; Jacket; Seismic; Push-over; Vulnerability.

1. Introduction

Recent earthquakes worldwide highlight the role of reinforced concrete (RC) bridges in maintaining the normal functionality of transportation. Post-event repair and restoration not only lead to direct economic losses, but indirect losses arising from network down time, traffic delay and business interruption. An unavoidable reality is that the majority of highway and urban RC bridges were completed several decades ago. The inappropriate design or detailing and the deterioration in performance necessitate the seismic retrofit of these RC bridges, to meet the current performance-based seismic design specifications [1,2].

Extensive researches involve in seismic retrofitting of a RC bridge pier and traditional techniques include RC jackets [3,4], steel jackets [5~7] and FRP wrappings [8,9]. Alongside, many scholars devote to retrofitting techniques with novel materials, i.e., cement-based matrices with textile reinforcement [10~12], engineered cementitious composites [13,14], and high-performance fiber-reinforced cementitious composite [15].

Exhibiting agreed compressive and tensile strengths, excellent toughness, and apparent energy dissipation capacity [16,17], ultrahigh-performance concrete (UHPC) appears as a potential alternative option to enrich the retrofitting techniques. As one of cementitious materials, UHPC was found compatible with normal-strength concrete [18]. Dagenais et al. [19] indicated that UHPC eliminated brittle bond failure in the lap splice region, which frequently occurred in the RC piers built in the USA prior to the 1970s. Xu et al. [20] pointed out UHPC piers were more ductile than their RC counterparts.

In this study, the authors focus on the retrofitting effectiveness of "as-built" low flexural strength bridge piers with the UHPC jacket. The enhancement of a pier's shear strength is out of the scope and will be investigated in the future. The main purposes of the retrofitting work are: (1) rising the flexural strength, and (2) enhancing the seismic resilience by reducing the concrete damage and the residual drift. To this end, the mono-wide-strip UHPC (W-UHPC) jacket is proposed to rise the pier's flexural strength, by enlarging the cross-section of the shaft by the W-UHPC jacket, see Fig.1a. Furthermore, the authors also propose the multi-narrow-strip UHPC (N-UHPC) jacket which does not alter the dimensions of the shaft. With the interface opening between the UHPC strips and the shaft (see Fig.1b), the N-UHPC jacket is expected to eliminate the concrete cracking, spalling and crushing, which frequently occur in an "as-built" bridge pier subject to strong ground motion. Cyclic quasi-static loading was performed on five rectangular RC piers, including one prototype pier, two piers retrofitted with the W-UHPC jacket, and the other two piers retrofitted with the N-UHPC jacket. Their seismic responses were compared, including strength, stiffness, energy dissipation, self-centering, damage, etc.

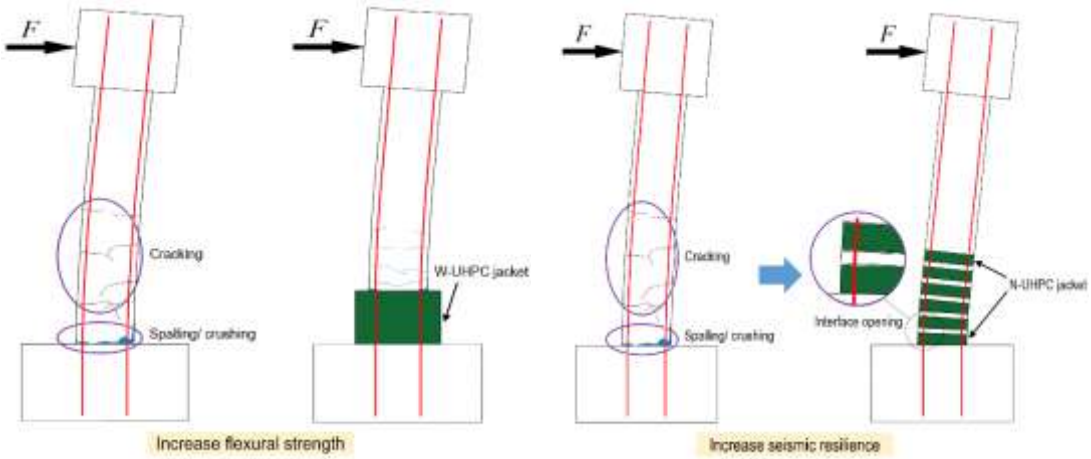

(a) The W-UHPC jacket. (a) The N-UHPC jacket.

Fig. 1. The retrofitting purposes.

2 Experimental programs

2.1 Specimen design and fabrication

Five 1:2 scaled low strength bridge RC piers were firstly fabricated, with identical dimensions and reinforcements. One pier served as the benchmark. All "as-built" piers owned a 0.70×0.80×0.70m top cap, a 0.45×0.50×2.30m shaft, and a 0.90×0.70×1.30m footing, see Fig.2. During the test, the lateral displacement-control load was applied at the middle of the top cap, and the footing was fixed to the ground. The height-to-width ratio for pier UR was (2.30+0.70/2)/0.5=5.3. To represent RC piers with low flexural strength, the longitudinal reinforcement percentage 0.71% was deliberatively selected, realized by eight 16mm ribbed HRB400 rebars. The 8mm plain HPB300 rebars served as the stirrups, and spaced at a distance of 80 mm in the plastic hinge zone, see Fig. 2.

Table 1. Design parameters for the tested piers.

Pier ID	Jacket		Longitudinal rebar	Stirrup	N
	W-UHPC	N-UHPC			
UR			Eight C16 HRB400	A8 HPB300: @80 mm at two ends; @160 mm at middle.	0.08 $f_c'A_g$
W400	√				
W850	√				
N3		√			
N6		√			

Note: N - external axial load; f_c' - cylindrical strength of concrete; A_g - cross-section area.

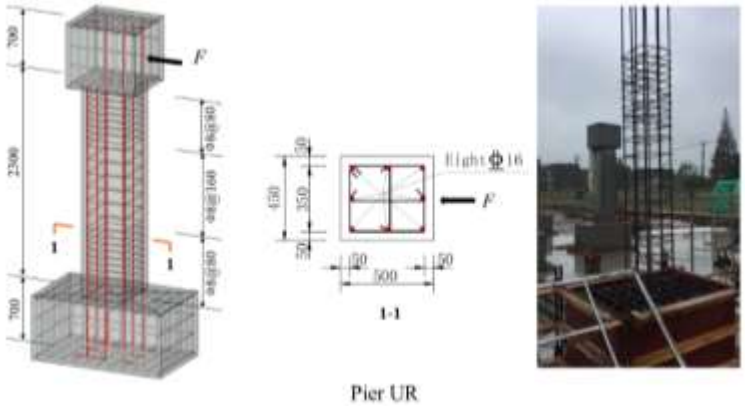

Fig. 2. Geometry and reinforcement details of pier UR.

After 28-day natural curing, two "as-built" piers were subsequently retrofitted with the W-UHPC jackets, see Fig.3 and Table 1. The common thickness for a RC jacket is greater than 100mm. Anchored at the enhanced compressive and tensile strengths, the thickness of the W-UHPC jackets was deliberatively selected as 50mm. To probe the influences of a jacket's height on the seismic responses, the 400mm-height ($\approx 1\,L_p$) and the 850 mm-height ($\approx 2\,L_p$) W-UHPC jackets were employed, where L_p =393 mm was the height of the "as-built" pier's plastic hinge zone and was evaluated by Seismic Design Criteria 1.7 [1]. To well bond the W-UHPC jacket to the shaft, roughness treatment was implemented at the normal-strength concrete's surface. Attention was paid that proper humidity should be maintained at the roughened surface when casting the UHPC [18].

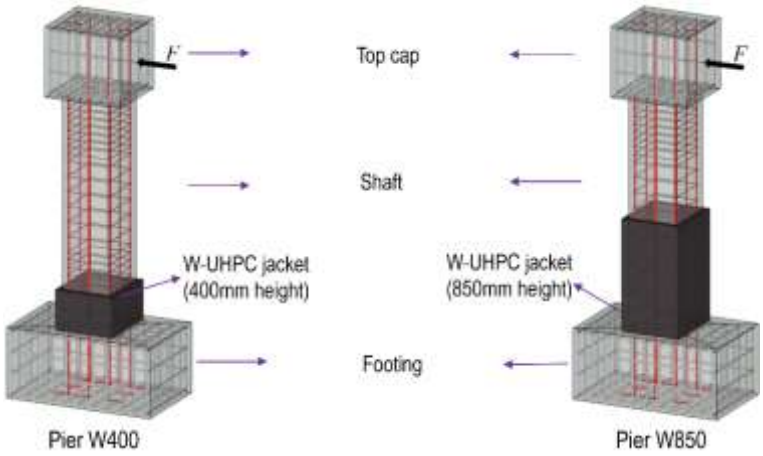

Fig. 3. Piers W400 and W850.

In contrast, another two "as-built" piers were retrofitted with the N-UHPC jackets, see Fig.4 and Table 1. Different from the W-UHPC jacket which enlarged the cross-section of the base shaft, the N-UHPC jacket remained the cross-section consistent. The height and thickness of one UHPC strip were 100mm and 50mm, respectively, and the height of normal-strength concrete between two UHPC strips was 50mm. Consequently, three and six UHPC strips leaded to 400mm($\approx 1\,L_p$) height retrofitting zone for pier N3, and 850mm($\approx 2\,L_p$) height retrofitting zone for pier N6, respectively. The sequences for retrofitting the "as-built" piers with N-UHPC jackets was a little complicated, with respect to the W-UHPC jackets. At the first step, the parts of normal-strength concrete were removed. Unfortunately, the authors found that the grouting quality of UHPC was hard to be guaranteed.

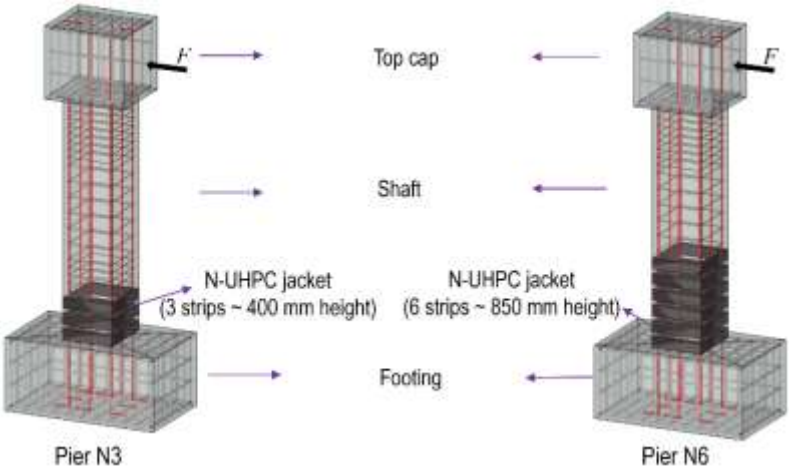

Fig. 4. Piers N3 and N6.

2.2 Material properties

The normal-strength concrete owned the mean cubic compressive strength 44.2MPa, which was equivalent to the mean cylindrical compressive strength 34.9MPa. Three samples for HRB400 ribbed reinforcement steel were tensioned and the mean yielding strength 432 MPa was obtained, as well as the mean peak strength 576 MPa.

The UHPC was the commercial product from Sobute New Materials CO., LTD, and the mixture proportions for one cubic meter UHPC was 2095.0kg power, 156.0kg 0.2mm-dia. steel fiber, 22.1kg

superplasticizer, and 182.4kg water. Steel fibers distributed randomly and had 2600MPa tensile strength, 205GPa elastic modulus, 7840kg/m3 density, and 20mm length. The mean cubic compressive strength of the UHPC after 28-day natural curing was 129.7MPa, which was equivalent to mean cylindrical compressive strength of 102.5MPa. Elastic modulus for the UHPC was around 57.0GPa. Two custom-fabricated dog-bone specimens were tensioned uniaxially and the mean tensile strength for the UHPC was 7.81MPa.

2.3 Test setup

Before cyclic loading, the vertical axial load equal to 8% of the RC pier's ultimate compressive strength was applied, through hydraulic jacks and pre-tensioned thread bars. Cyclic lateral loading was applied at the midpoint of the RC cap, using a 6000kN MTS electrohydraulic servo machine. The magnitudes of the loading force and the horizontal displacement at loading point were precisely monitored by the MTS experiment system. Displacement-control loading scheme is illustrated as Fig.5. Three repeated cycles were performed at each loading phase. The amplitude increment was set as 5mm for the cycles with amplitude lesser than 50mm. The amplitude was subsequently amplified to 10mm, until the termination of the test.

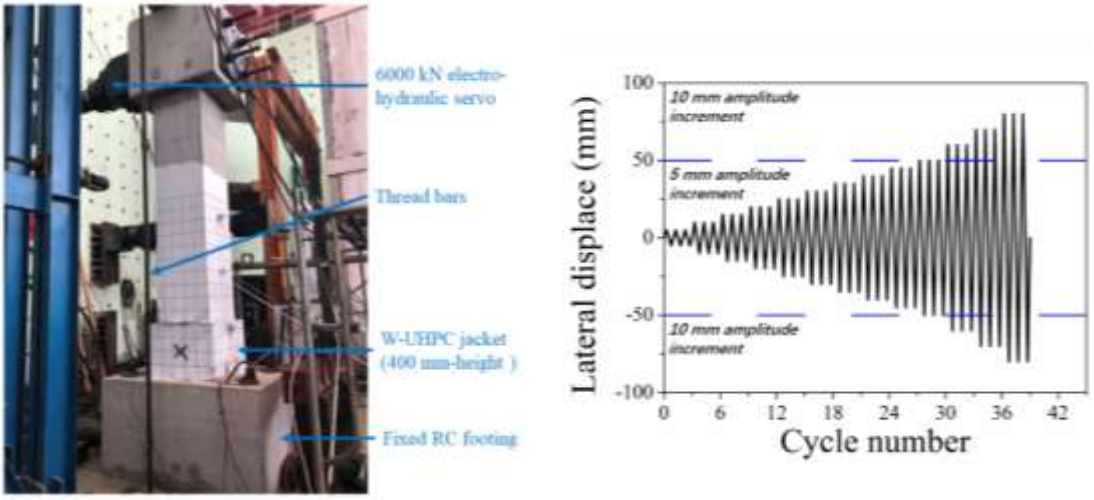

Fig. 5. Test setup for pier W400 and loading scheme.

Two issues were encountered when loading the piers. At a large lateral displacement, the bars elongated and leaded to the increase of the vertical axial load vertical axial load N. To eliminate the disturbance, oil pressures of the two hydraulic jacks were manually controlled as approximately a constant value. Consequently, the variation of the recorded tensile force in the two bars was within 5%. Alongside, the inclination of thread bars leaded to a trace of horizontal restoring force. The recorded lateral displacement-force relationship from the MTS system was revised to eliminate the disturbance.

3 Global damage evolutions

3.1 Pier UR

Tested hysteretic curve for pier UR is shown in Fig.9, the hysteretic response appeared quite symmetric for push/pull cycles. Damage evolutions with the lateral drift δ is shown in Fig. 6 and summarized in Table 2.

Table 2. Overview of pier UR's damage evolutions.

Drift (%)	Damage description
0.75	Multiple flexural cracks emerged, propagated and widened.
1.89	Flexural cracks stabilized; Concrete slightly spalled at the extreme fiber of compressive toe.
2.26	Arrived at peak lateral strength F_p.
3.40	Flexural cracks widened; Evolution of concrete spalling at end of the RC shaft.
3.77	**Lateral strength dropped to 0.8 F_p.**
4.15	Height of spalling was 0.2 m; Fracture of the longitudinal rebar.

Flexural-dominated failure mode was observed. Due to the low flexural reinforcement ratio, no crushing was observed for the core concrete enclosed by the stirrups. After the termination of the test, damage patterns at δ=4.15% are presented as the photo in Fig.9. The height of concrete spalling reached 0.2 m.

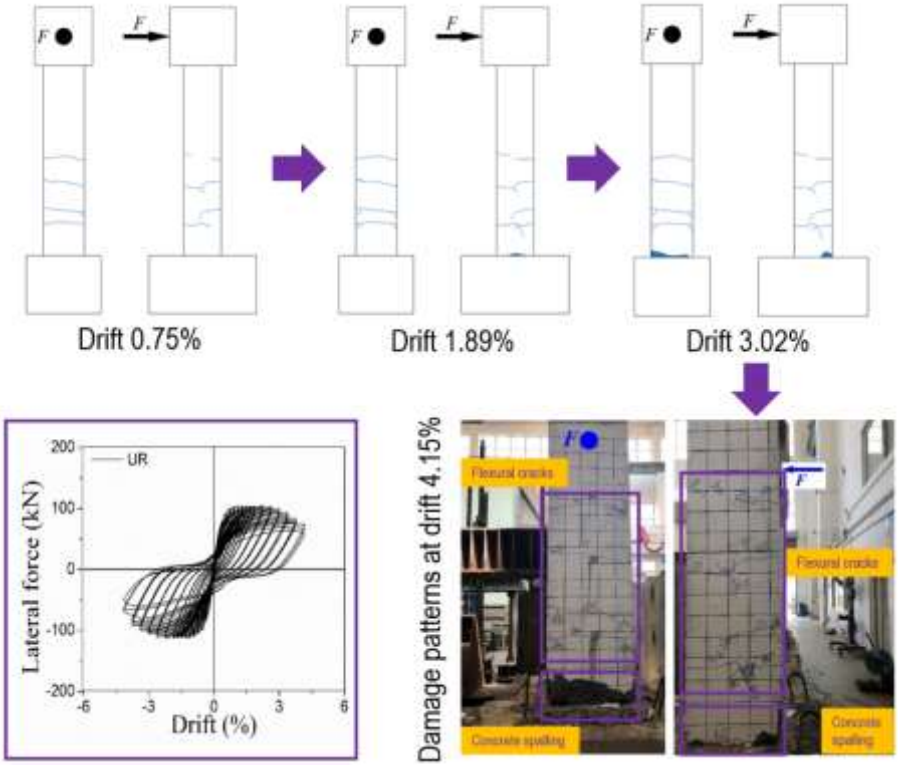

Fig. 6. Damage evolutions and hysteretic curve and for pier UR.

3.2 Pier W400

Due to limitations of the MTS electrohydraulic servo machine, pier W400 was cyclically loaded until δ=4.91%, without the fracture of the longitudinal rebar. To remedy the test, monotonic pushover was then performed for pier W400. The fracture of the longitudinal rebar occurred at the interface between the W-UHPC jacket and the footing, and flexural-dominated failure mode was observed.

Table 3. Overview of pier W400's damage evolutions.

Drift (%)	Damage description

0.75	Flexural cracks emerged, propagated and widened;
1.70	Corner of the RC shaft spalled above the W-UHPC jacket; Vertical expansive cracks occurred on the W-UHPC jacket; Gap-opening was witnessed between the W-UHPC jacket and the RC footing.
2.26	Arrived at peak lateral strength F_p.
2.64	More vertical expansive cracks occurred on the W-UHPC jacket; Flexural cracks on the RC shaft stabilized; Gap-opening increased.
3.40	Diagonal shear cracks propagated on the side faces of the W-UHPC jacket. Gap-opening increased to 7~8 mm.
4.91	**Lateral force dropped below 0.8 F_p,** but no fracture of the longitudinal rebar.

The higher elastic modulus and tensile strength of UHPC passively confined the lateral expansion of the shaft, which was indicated by the massive vertical expansive cracks on the 400mm-height W-UHPC jacket. The integrity of the retrofitted RC pier was enhanced and spalling or crushing were not observed, either for the W-UHPC jacket or the normal-strength concrete shaft.

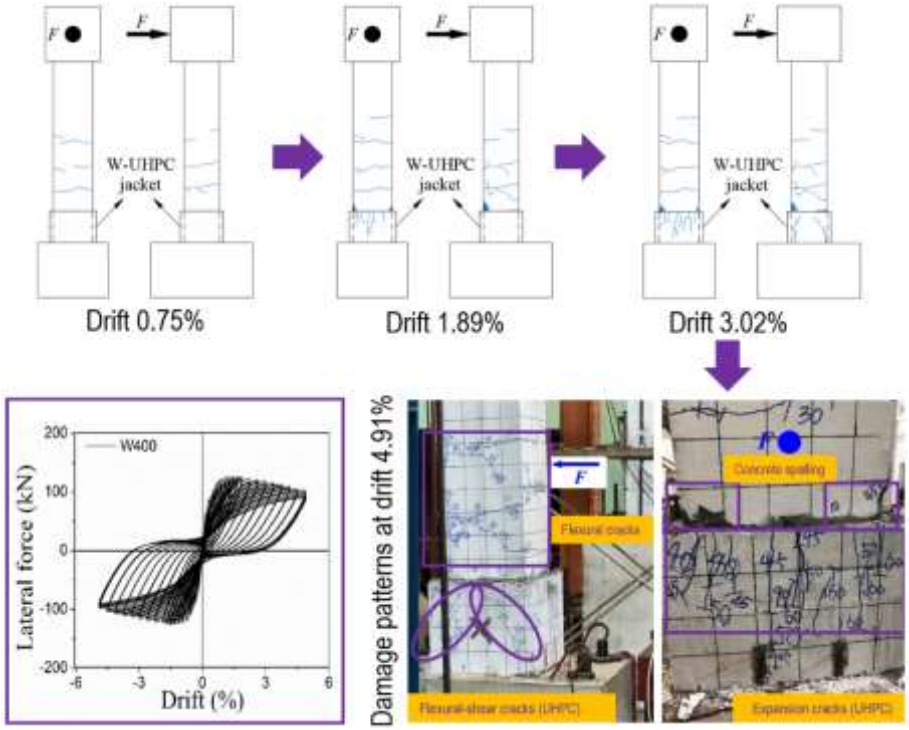

Fig. 7. Damage evolutions and hysteretic curve and for pier W400.

3.3 Pier W850

Tested hysteretic curve for pier W850 is shown in Fig.8. Damage evolutions with the lateral drift δ is shown in Fig.8 and summarized in Table 4.

Table 4. Overview of pier W850's damage evolutions.

Drift (%)	Damage description
0.75	Flexural cracks emerged, propagated and widened.

1.13	Gap-opening was witnessed between the W-UHPC jacket and the RC footing.
1.70	Flexural crack of the RC shaft stabilized; Gap-opening increased to 4 mm.
1.89	Vertical expansive cracks occurred at the UHPC jacket.
2.64	Arrived at peak lateral strength F_p.
3.40	Gap-opening increased to 12 mm.
3.77	**Fracture of the longitudinal rebar;** Gap-opening increased to 14 mm.

Flexural-dominated failure mode was observed. Damage patterns at δ=3.77% are presented as the photo in Fig.8. Similar to pier W400, vertical expansive cracks indicated the passive confinement effect from the W-UHPC jacket. Due to the greater height, the 850 mm-height jacket itself displayed lesser expansive cracks. No spalling or crushing were observed, either for the W-UHPC jacket or the normal-strength shaft.

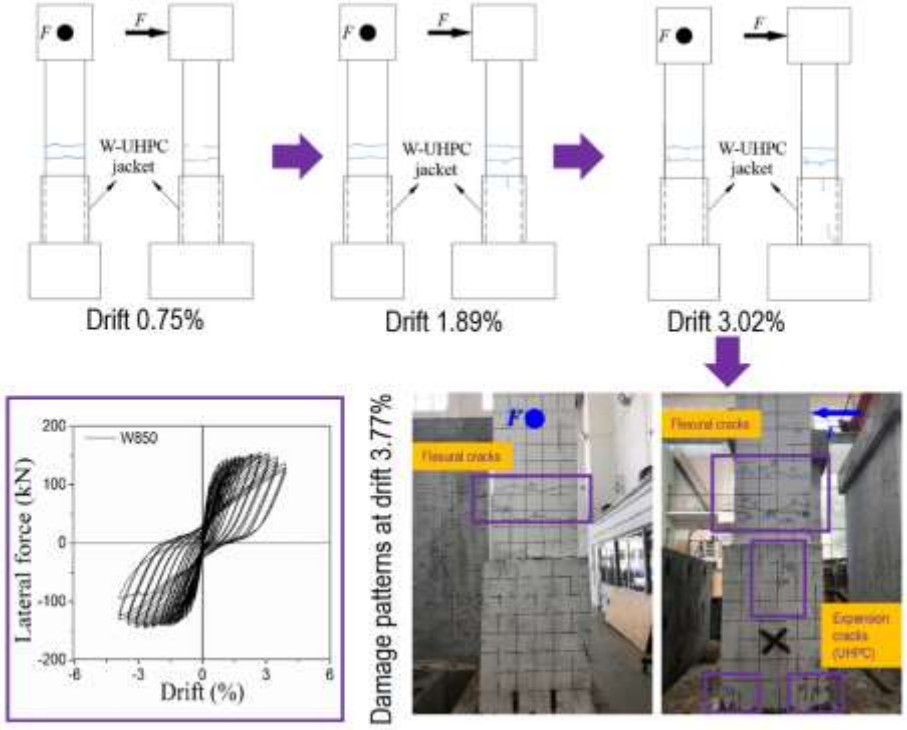

Fig. 8. Damage evolutions and hysteretic curve and for pier W850.

3.4 Pier N3

Pier N3 was also not loaded to the fracture of the longitudinal rebar, due to the limitations of the MTS electrohydraulic servo machine. Tested hysteretic curve for pier N3 is shown in Fig.9. Damage evolutions with the lateral drift δ is shown in Fig.9 and summarized in Table 5.

Table 5. Overview of pier N3's damage evolutions.

Drift (%)	Damage description
0.38	Interfaces between upper surfaces of UHPC strips and the RC shaft opened.
1.13	Interface-opening widened; Multiple flexural cracks were witnessed in the RC shaft.

1.32	Vertical expansive cracks formed on the N-UHPC jacket; Arrived at peak lateral strength F_p.
1.89	Flexural cracks stabilized; Interface-opening reached 7 mm.
3.39	Fracture of one stirrup at the middle UHPC strip; Breakage of the middle UHPC strip.
3.77	**Lateral force dropped below 0.8 F_p.**
4.15	Termination of the test, although no fracture of the longitudinal rebar.

Flexural-dominated failure mode was observed. Damage patterns at δ=4.15% are presented as the photo in Fig.9. Vertical expansive cracks on the N-UHPC jacket clearly indicated its passive confinement effect on restraining the lateral deformation of the normal-strength shaft. Due to the construction deficiency, there existed a seam between the upper surface of the UHPC strip and the shaft. The seam weakened the passive confinement effect of the UHPC strip. The compressive buckling of longitudinal rebars was not well suppressed and leaded to the fracture of one stirrup at δ=3.39%, as well as the UHPC strip.

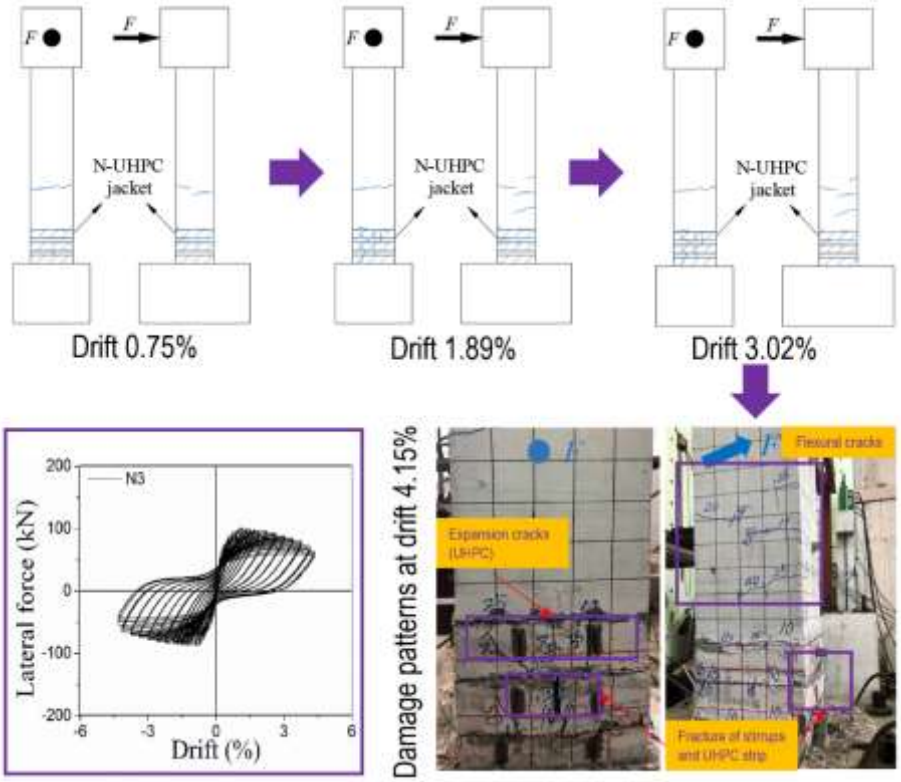

Fig. 9. Damage evolutions and hysteretic curve and for pier N3.

3.5 Pier N6

Tested hysteretic curve for pier N6 is shown in Fig.10. Damage evolutions with the lateral drift δ is shown in Fig.13 and summarized in Table 6.

Table 6. Overview of pier N6's damage evolutions.

Drift (%)	Damage description
1.13	Interfaces between upper surfaces of UHPC strips and the RC shaft opened; Flexural cracks emerged at the RC shaft.

1.51	Flexural cracks stabilized.
2.26	Interface-opening widened; Arrived at peak lateral strength F_p.
4.15	**Fracture of the longitudinal rebar.**

Flexural-dominated failure mode was observed. Final damage distribution at δ = 4.15% is presented as the photo in Fig.10. If retrofitted with accepted quality, the passive confinement effect enabled pier N6 to remain overall integrity, and no spalling or crushing were observed, either for the N-UHPC jacket or the shaft. Moreover, there were no compressive buckling of the longitudinal rebar and no fracture of the stirrup.

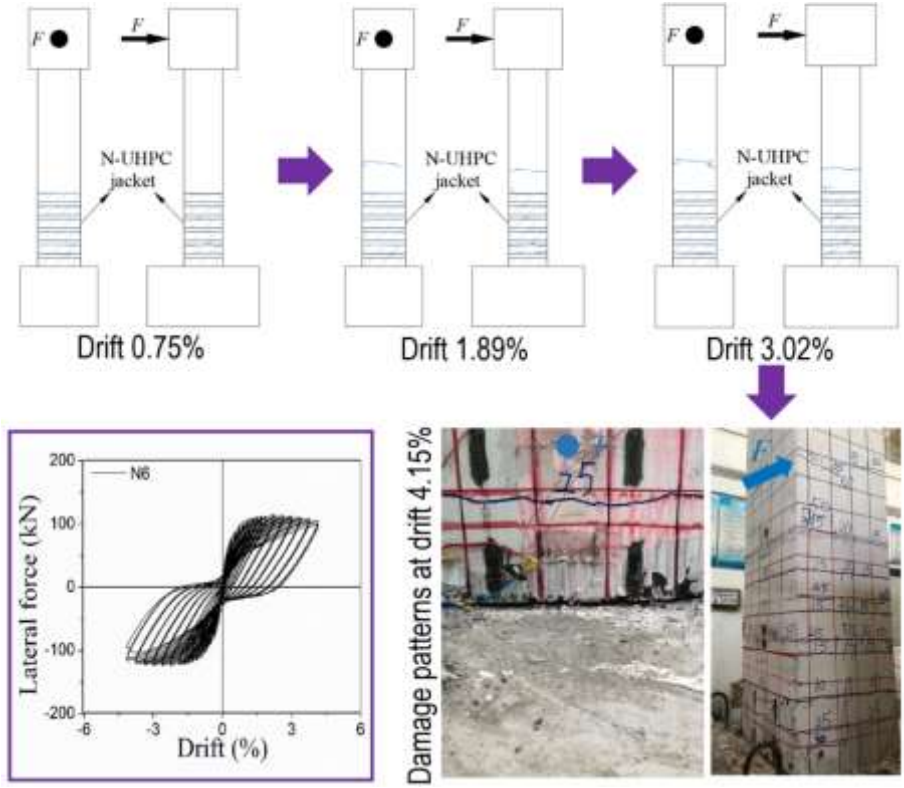

Fig. 10. Damage evolutions and hysteretic curve and for pier N6.

3 Summary and final remarks

Five scaled bridge piers were tested to quantitively evaluate the novel retrofitting method adopting the W-UHPC and N-UHPC jackets. Relying on the experiment results, seismic vulnerability of these five piers is subsequently evaluated. The following conclusions can be drawn:

(1) The W-UHPC jacket was effective in enhancing the flexural strength. The passive confinement, cross-section enlargement, and gap-opening effects were witnessed for piers W400 and W850. With proper selection of the W-UHPC jacket's height, pier W400 gained apparently rise in the ductility and energy dissipation capacity. Alongside, proper design of the W-UHPC jacket should be paid to avoid the potential relocation of the plastic hinge zone.

(2) The N-UHPC jacket was effective in mitigating the pier's concrete cracking, spalling and crushing. Moreover, residual drifts of piers N3 and N6 were also reduced. The passive confinement and interface-opening effects were witnessed for the piers retrofitted with the N-UHPC jacket. However, guaranteeing the construction quality is critical for the N-UHPC jacket.

The current research serves as a pilot investigation and focuses on the seismic retrofitting of low flexural strength rectangular bridge piers with the W-UHPC and N-UHPC jackets, which are typical piers completed in China prior to the 1980s. Further researches are needed to comprehensively investigate the potentials of the UHPC jacket in retrofitting the bridge piers.

4 References

[1] SDC (The Seismic Design Criteria) (2013): Caltrans seismic design criteria version 1.7. *California Department of Transportation. Sacramento, CA, USA.*

[2] JTG D60 Ministry of Communication (MOC) of China (2004): General code for design of highway bridges and culverts.

[3] Priestley MN, Seible F, Calvi GM (1996): *Seismic design and retrofit of bridges*. John Wiley & Sons.

[4] Rodriguez M, Park R (1994): Seismic load tests on reinforced concrete columns strengthened by jacketing. *Structural Journal*, *91*(2), 150-159.

[5] Priestley MN, Verma R, Xiao Y (1994): Seismic shear strength of reinforced concrete columns. *Journal of structural engineering*, *120*(8), 2310-2329.

[6] Ghasemi H, Otsuka H, Cooper JD, Nakajima H (1996): Aftermath of the kobe earthquake. *Public Roads*, *60*(2).

[7] Itani R (2003): Effects of retrofitting applications on reinforced concrete bridges. *Columns*.

[8] Seible F, Priestley MN, Hegemier GA, Innamorato D (1997): Seismic retrofit of RC columns with continuous carbon fiber jackets. *Journal of composites for construction*, *1*(2), 52-62.

[9] Foraboschi P (2016): Effectiveness of novel methods to increase the FRP-masonry bond capacity. *Composites Part B: Engineering*, *107*, 214-232.

[10] Ilki A, Demir C, Bedirhanoglu I, Kumbasar N (2009): Seismic retrofit of brittle and low strength RC columns using fiber reinforced polymer and cementitious composites. *Advances in Structural Engineering*, *12*(3), 325-347.

[11] Bedirhanoglu I, Ilki A, Kumbasar N (2013): Precast fiber reinforced cementitious composites for seismic retrofit of deficient rc joints–A pilot study. *Engineering Structures*, *52*, 192-206.

[12] Ates AO, Khoshkholghi S, Tore E, Marasli M, Ilki A (2019): Sprayed Glass Fiber–Reinforced Mortar with or without Basalt Textile Reinforcement for Jacketing of Low-Strength Concrete Prisms. *Journal of Composites for Construction*, *23*(2), 04019003.

[13] Li VC, Horii H, Kabele P, Kanda T, Lim YM (2000): Repair and retrofit with engineered cementitious composites. *Engineering Fracture Mechanics*, *65*(2-3), 317-334.

[14] AL-Gemeel AN., Zhuge Y (2018): Experimental investigation of textile reinforced engineered cementitious composite (ECC) for square concrete column confinement. *Construction and Building Materials*, *174*, 594-602.

[15] Cho CG, Han BC, Lim SC, Morii N, Kim JW (2018): Strengthening of reinforced concrete columns by high-performance fiber-reinforced cementitious composite (hpfrc) sprayed mortar with strengthening bars. *Composite Structures*, *202*, 1078-1086.

[16] Nagayama M, Miyashita T (2008): Tensile Stress-Strain Relationship of High-Performance Fiber Reinforced Cement Composites. In *14th World Conference on Earthquake Engineering*.

[17] Park SH, Kim DJ, Ryu GS., Koh KT (2012): Tensile behavior of ultra high performance hybrid fiber reinforced concrete. *Cement and Concrete Composites*, *34*(2), 172-184.

[18] Aaleti S, Sritharan S, Abu-Hawash A (2013): Innovative UHPC-normal concrete composite bridge deck. In *Proceedings of the RILEM-fib-AFGC International Symposium on Ultra-High Performance Reinforced Concrete, Eds: F. Toutlemonde, J. Resplendino, Rilem Publications SARL, Bagneux, France*.

[19] Dagenais MA, Massicotte B, Boucher-Proulx G (2017): Seismic retrofitting of rectangular bridge piers with deficient lap splices using ultrahigh-performance fiber-reinforced concrete. *Journal of Bridge Engineering*, *23*(2).

[20] Xu S, Wu C, Liu Z, Han K, Su Y, Zhao J, Li J (2017): Experimental investigation of seismic behavior of ultra-high performance steel fiber reinforced concrete columns. *Engineering Structures*, *152*, 129-148.